CHAPTER 28

SELF-LOCALIZATION OF UAV FORMATIONS USING BEARING MEASUREMENTS

Iman Shames,[1] Barış Fidan,[2] Brian D. O. Anderson,[1] and Hatem Hmam[3]

[1]The Australian National University and The University of Melbourne

[2]University of Waterloo, Waterloo, Canada

[3]Defence Science and Technology Organisation, Edinburgh, Australia

THIS CHAPTER begins by treating a localization problem recently encountered in an operational context; that is, localizing three agents moving in a plane when the interagent distances are known, and in addition, the angle subtended at each agent by lines drawn from two landmarks at known positions is also known. It is shown as a key conclusion that there are in general a finite number greater than one of possible sets of positions for the three agents. In addition, the generalization of the result for more than three agents is presented. Examples are presented to show the applicability of the methods proposed here.

28.1 INTRODUCTION

In many multiagent applications, it is desired to know the positions of the agents. For example, in bushfire surveillance or a search-and-rescue operation, sensing the data without knowing the position of the sensing agents is not enough to accomplish the task at hand. A trivial solution to this problem is to install global positioning systems (GPSs) on each agent. However, when GPS signals are lost or corrupted [1], or when the agents operate indoors, use of GPSs for localization purposes may

Handbook of Position Location: Theory, Practice, and Advances, Second Edition.
Edited by S. A. (Reza) Zekavat and R. Michael Buehrer.

Published 2019 by John Wiley & Sons, Inc.
Companion Website: www.wiley.com/go/zekavat/positionlocation2e

be infeasible or limited [2]. Thus, it is imperative to design other methods for estimating the positions of the sensing agents when a GPS signal is not available. There are also many other scenarios when GPS signals are not available. Examples include outer space localization and localization on the surface of other planets. The vehicle itself can serve as a pair or more of landmarks, which the robots can use for absolute navigation and referencing, as long as the vehicle remains in the line of sight (LOS) of the robot.

In the literature, there are many methods that achieve the task of localizing agents via measuring distances [3, 4], time difference of arrival [5], and direction of arrival (DOA) [6].

In this chapter, we address the localization problem where self-localization is achieved cooperatively among a team of bearing and distance sensing agents (e.g., unmanned aerial vehicles [UAVs] or robots) and where the position information of the two landmarks is available, as are either interagent distances or the bearings measured to each agent of the agents in the formation.

The problem considered here is very similar to the problems considered in [6–10]. The cooperative localization task is then to put the pieces of information together, for example, interagent distances, subtended angles, and landmark positions, and localize the agents. Note here that the localization is to be achieved instantaneously; we are not envisaging collecting information from agents at a number of successive instants of time and using them to infer position at a single instant of time (the connection with Kalman filtering is explored further below). In the distance-based localization literature, the nodes with known position are called anchors (beacons) [11], and since each anchor is determined exactly, they can be considered as anchors as well. Due to the nature of the problem mentioned above, these anchors are collinear. However, the results obtained in this chapter are not limited to collinear anchors and can be applied to scenarios with arbitrary arrangement of the anchors. Note also that we later extend the results to systems with more than three agents capable of measuring the subtended angle by the landmarks.

It is shown in this chapter that the solution count for the above localization problem (involving three agents) is less than 12. If there is no unique solution, then what is the point of this analysis? There are in fact several ways in which it can be relevant. First, GPS data may be intermittently available to an agent. When it is available, localization is obviously unique. When it ceases to be available, the fact that the agents are moving continuously with their initial position known means that there will be a basis for making the correct selection out of a finite number of localization possibilities at subsequent times.* Second, given that the number of possible solutions to the localization problem is finite, it may be that additional very crude data indeed (e.g., agent T' is located in this general region) will be enough to disambiguate the multiple solutions. Third, if more agents are available, then the additional information will generically allow unique localization, and indeed, when measurements are noisy, will in general allow some amelioration of the distorting effects of the noisy measurements. Lastly, the method described in this chapter can

*At least until the agents move to positions corresponding to a double solution of the localization problem, after which two tracks would have to be followed assuming no disambiguating information.

be considered as batch processing of the agent locations serving to initialize and improve the updates of a Kalman-based filter that tracks the agent positions as the agents move in their environment. Kalman-based filters are also prone to errors when the agent's motion model deviates significantly from the actual agent motion. Our batch processing method can guard against such behavior and reinitialize the filter.

There is a vast body of literature using Bayesian methods that deals with localization problems. For example, in [12], a collective localization problem based on Kalman filtering is proposed, and [13] uses a Gaussian sum filter to solve the initialization problem in bearing-only simultaneous localization and mapping (SLAM). Differently from these approaches, the tools for obtaining our results are drawn from two nonconventional sources. The first is the theory of rigid graphs (see, e.g., [14–17]). In recent years, its relevance to localization of sensor networks has come into prominence [11, 18]. A good deal of the theory of rigid graphs deals with the question of when localization is possible [19, 20]. The second source we draw on is the mechanical engineering literature dealing with four-bar linkage mechanisms [21, 22]. As it turns out, this literature has developed ideas for describing the loci of points that are part of a planar mechanism made up from pin joints and rigid bars that provide distance constraints between the joints. Moreover, for the purposes of this chapter, we assume that we have access to noiseless interagent distance measurements. The significance of considering the noiseless scenario is that it equips us with a knowledge on the number of solutions to the problem and methods to calculate these solutions, where later methods to deal with noisy case are built upon.

The outline of this chapter is as follows. In the next section, we formally set up the problem. In Section 28.3, we first introduce the results related to network localization in the field of rigidity and then establish the connection of the problem described in Section 28.2 with the rigidity theory. In Section 28.4, we study four-bar linkage mechanisms, and in Section 28.5, we propose a solution to the problem of interest using the mathematical methods developed to analyze these mechanisms. In Section 28.6, we consider the localization problem for formations with a larger number of agents than initially conisdered. In Section 28.7, we study the situation where information about an extra landmark is available. In Section 28.8, we introduce another localization scenario where the agents can measure all the subtended angles (not only at the landmarks). Concluding remarks come at the end.

28.2 PROBLEM SETUP

The arrangement to be considered, and the one on which the later developments are based, is depicted in Figure 28.1. Specifically, we consider n mobile agents (in this case, $n = 3$), designated T_1, T_2, and T_3, that are to be localized. The agents detect two landmarks located at positions L_1 and L_2, which are known to the agents. The landmarks can be radars, radio frequency (RF) beacons, or some visible features if an imaging sensor is used. Each agent collects the bearing angle information to each of the landmarks. *However, with no GPS information (no knowledge about the absolute heading reference), there is no absolute heading reference for each agent, and the bearing angle information cannot be used directly for localization purposes.*

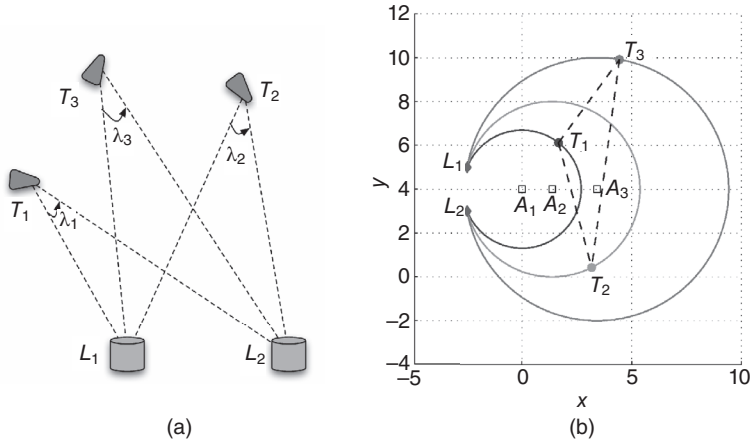

Figure 28.1 The localization problem setting and the agents loci. (a) Landmarks L_1, L_2, formation $T_1T_2T_3$, and angles λ_i in Problem 1. (b) Agent loci for a sample setting.

Nevertheless, using the angle difference (i.e., the difference between two bearings), the need for knowing the heading is removed. This angle difference is the angle subtended at each agent by the two landmarks (λ_i, $i = 1,2,3$) (see Fig. 28.1) and knowing its value. It is straightforward from the inscribed angle theorem to determine that each agent i is located on a circle of known center, A_i, and radius, R_i, that passes through the two landmarks. Note that both values of A_i and R_i can be determined by λ_i and the landmark positions. The centers, A_i ($i = 1,2,3$), lie on the perpendicular bisector of the line joining the two landmarks. A priori information is assumed to be available that positions all agents on the same known side of the line joining the two landmarks. This can be ensured by choosing landmarks on the boundary of the agents region of operation.

We adopt the naming convention from the distance-based localization literature and call the points with the known positions anchors (beacons) [11]. Since each A_i is determined exactly (from the knowledge of positions of the landmarks and the angles λ_i), they can be considered as (pseudo-)anchors as well. Due to the nature of the problem mentioned above, these anchors are collinear. However, the results obtained in this chapter are not actually limited to collinear anchors and can be applied to scenarios with arbitrary arrangement of the anchors. First, we formalize the definition of the *underlying graph* of a formation.

***Definition 1 (Underlying Graph of a Formation)*:** A formation of point agents in the plane, $\mathcal{F}$, can be represented by a graph $\mathcal{G}(\mathcal{V}, \mathcal{E})$, with vertex set $\mathcal{V}$ and edge set $\mathcal{E}$; the vertices in $\mathcal{V}$ correspond to the agents, and an edge in the graph exerts between two vertices $v_1, v_2 \in \mathcal{V}$ only when the distance between the corresponding agents of the formation is known. We call $\mathcal{G}$ the underlying graph of $\mathcal{F}$.

We can generalize the problem described above as the following problem.

***Problem 1*:** Consider a formation $\mathcal{F}$ with the underlying graph $\mathcal{G}(\mathcal{V}, \mathcal{E})$, where $\mathcal{V} = \mathcal{T} \cup \mathcal{A}$ is the set of vertices with $\mathcal{T} = \{T_1,T_2,T_3\}$, $\mathcal{A} = \{A_1,A_2,A_3\}$. The agents in $\mathcal{A}$ are known as anchors, and those in $\mathcal{T}$ as targets. Furthermore, $\mathcal{E} = \{T_1T_2,T_1T_3,T_2T_3, A_1A_2,A_1A_3,A_2A_3,A_1T_1,A_2T_2,A_3T_3\}$ is the set of edges. Knowing the exact length of all edges in $\mathcal{E}$, and the exact positions of the anchors,

(i) Can one localize the targets, uniquely, or to one of a finite number of sets of positions?

(ii) If so, what are the possible localization solutions?

***Remark 1*:** In this problem there is no assumption of collinearity of A_i, $i = 1,2,3$. The case where A_i are collinear can be treated as a special case of this problem.

In the sequel, we propose an answer to the first question posed in Problem 1. However, first we introduce some basic concepts from rigidity theory and its relationship to the localization problem.

28.3 A RIGID GRAPH THEORETICAL FRAMEWORK FOR FORMATION LOCALIZATION

In this section, we review some aspects of the problem of localizing, that is, determining the positions of agents in a formation where a number of interagent distances are known, and additionally, some absolute position data is available. We appeal to the literature on rigid graph theory and its application to sensor network localization [11, 18–20].

***Definition 2 (Graph Realization Problem)*:** Consider a formation $\mathcal{F}$ with underlying graph $\mathcal{G}(\mathcal{V}, \mathcal{E})$. The task of assigning coordinate values to each vertex of a graph, $\mathcal{G}(\mathcal{V}, \mathcal{E})$, so that the Euclidean distance between any two adjacent vertices is equal to the edge length associated with the edge joining these two vertices, is the graph realization problem.

Given one solution to the graph realization problem, it is trivial that any translation, rotation, or reflection of this solution is another solution. All such solutions are congruent. Hence, it is relevant to ask whether there can be two solutions that are not congruent, and whether, disallowing translations, rotations, or reflections, the number of distinct solutions is finite or infinite. When there can be only one family of congruent solutions, one can say that the graph realization problem has a unique solution. This problem is also known as the problem of localizability in the literature (see [23] for more information).

Hendrickson [19] presents necessary conditions for a graph to be uniquely realizable in $\mathbb{R}^2$, that is, with one family of congruent solutions, and the same conditions were proved later by Jackson and Jordan [20] to be necessary and sufficient.

These conditions involve two concepts, namely redundant rigidity of a graph and three-connectedness of a graph. The concept of redundant rigidity requires a prior concept of rigidity, that is as follows.

***Definition 3 (Rigid Formations)*:** A formation $\mathcal{F}$ is called rigid if by explicitly maintaining distances between all the pairs of agents whose representative vertices are connected by an edge in $\mathcal{E}$, the distances between all other pairs of agents in $\mathcal{F}$ are consequentially held fixed as well.

The reader may refer to [14–16] for detailed information on rigid formations and rigidity.

***Definition 4 (Redundantly Rigid and Minimally Rigid Formations)*:** A redundantly rigid formation is one that remains rigid when any single edge constraint is removed. By way of contrast, a minimally rigid formation is one which ceases to be rigid when any single edge constraint is removed.

For the sake of simplicity, the underlying graph of a formation is called rigid, redundantly rigid, and minimally rigid if the formation is, respectively, rigid, redundantly rigid, and minimally rigid.

The notion $\mathcal{G}$ of a three-connected graph is standard (see, e.g., [24]). Such a graph has the property that between any two vertices, three nonintersecting paths can be found.

Jackson and Jordan's result [20] is as follows.

***Theorem 1*:** Consider a two-dimensional formation $\mathcal{F}$ with underlying graph $\mathcal{G}(\mathcal{V}, \mathcal{E})$. Then the graph realization problem is uniquely solvable for generic values of the formation edge lengths (interagent distances) if and only if $\mathcal{G}$ is redundantly rigid and three-connected.

From this result, we can have a definition for *globally rigid* graphs.

***Definition 5 (Globally Rigid Graphs)*:** A graph $\mathcal{G}$ with the two properties in Theorem 1, that is, redundant rigidity and three-connectedness, is termed globally rigid.

For a formation that is rigid but not globally rigid, one of at least of two ambiguities known as flip ambiguity or discontinuous flex ambiguity can occur [19]; these ambiguities are depicted in Figure 28.2. The reader may refer to [16] and [19] and

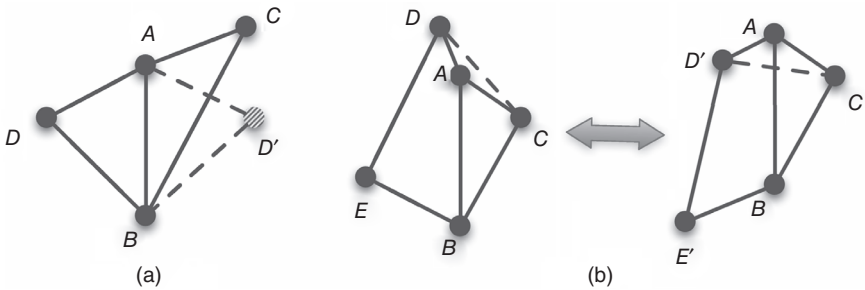

Figure 28.2 Illustration of (a) flip ambiguity: vertex D can be flipped over the edge (A, B) to a symmetric position D' and the distance constraints remain the same; (b) discontinuous flex ambiguity: temporarily removing the edge (C, D), the edge triple (D, A), (D, E), (E, B) can be flexed to obtain positions E' and D', such that the edge length (C, D) equals the edge length (C, D'), and then all the distance constraints are the same.

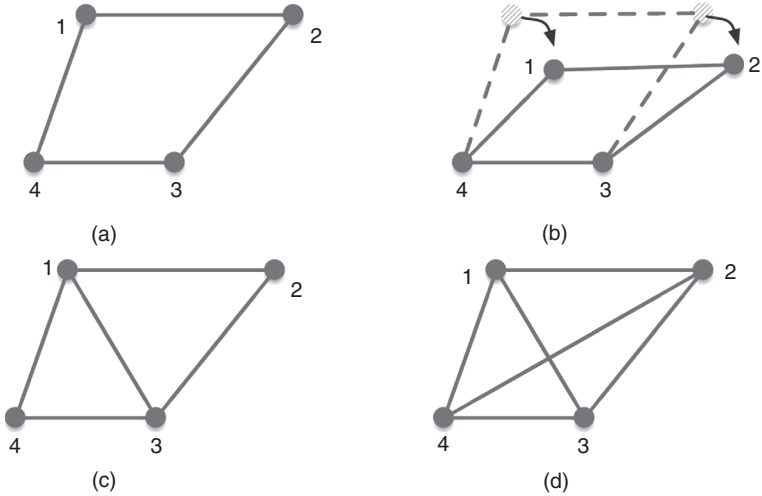

Figure 28.3 Rigid and nonrigid formations. The formation represented in panel (a) is not rigid. It can be deformed by a smooth motion without affecting the distance between the agents connected by edges, as shown in panel (b). The formations represented in panels (c) and (d) are rigid, as they cannot be deformed by any such move. In addition, the formation represented in panel (c) is minimally rigid because the removal of any edge would render it nonrigid. That of panel (d) is not minimally rigid; any edge may be removed without losing rigidity.

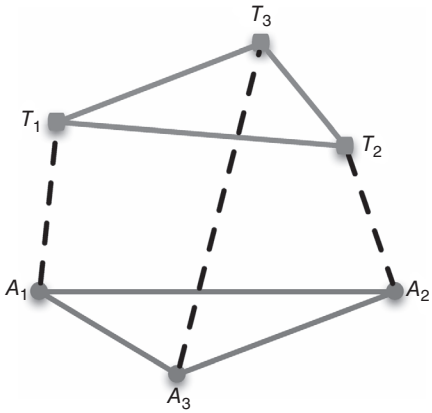

Figure 28.4 Graph representation of Problem 1.

references therein for further information on these ambiguities. Examples of nonrigid, rigid, and globally rigid graphs are presented in Figure 28.3.

Now we provide an answer the first question posed in Problem 1. An example of the formation $\mathcal{F}$ described in Problem 1 is depicted in Figure 28.4. A crucial concept pertinent to answering the first question posed in Problem 1 is a minimally rigid formation. Two ways are presented in the following paragraphs to see this fact.

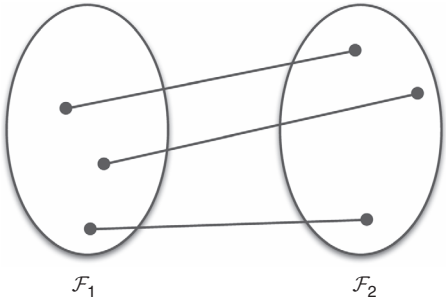

Figure 28.5 Setting described in Theorem 3.

Laman's Theorem [14]: Laman's theorem provides a combinatorial way to check rigidity, and indeed minimal rigidity. It requires the idea of an induced subgraph of a graph $\mathcal{G} = (\mathcal{V}, \mathcal{E})$. Let $\mathcal{V}'$ be a subset of $\mathcal{V}$. Then the subgraph of $\mathcal{G}$ induced by $\mathcal{V}'$ is the graph $\mathcal{G}' = (\mathcal{V}', \mathcal{E}')$, where $\mathcal{E}'$ includes all those edges of $\mathcal{E}$ that are incident on a vertex pair in $\mathcal{V}'$.

***Theorem 2 (Laman's Theorem [14])*:** A graph $\mathcal{G} = (\mathcal{V}, \mathcal{E})$ *in* $\mathbb{R}^2$ of $\mathcal{V}$ vertices and $\mathcal{E}$ edges is rigid if and only if there exists a subgraph $\mathcal{G}' = (\mathcal{V}, \mathcal{E}')$ with $2\mathcal{V}$-3 edges such that for any subset $\mathcal{V}''$ of $\mathcal{V}$, the induced subgraph $\mathcal{G}'' = (\mathcal{V}'', \mathcal{E}'')$ of $\mathcal{G}'$ obeys $\mathcal{E}'' \leq 2\mathcal{V}'' - 3$. It is minimally rigid if $\mathcal{E} = 2\mathcal{V} - 3$.

It is easy to check for the graph of Figure 28.4 that $\mathcal{E} = 2|\mathcal{V}| - 3$; one takes $\mathcal{G}' = \mathcal{G}$ and can verify the counting condition for all induced subgraphs.

Combination of Rigid Formations [17]: Another way of demonstrating minimal rigidity of a formation is by showing that it is a certain type of combination of two minimally rigid formations. The key theorem is as follows.

***Theorem 3 ([17])*:** Let $\mathcal{F}_1$ and $\mathcal{F}_2$ be two rigid formations, and consider a formation $\mathcal{F}$ formed by connecting these two formations with three edges, each edge incident on one vertex of $\mathcal{F}_1$ and one of $\mathcal{F}_2$, with no two edges incident on the same vertex. Then $\mathcal{F}$ is rigid. Moreover, if $\mathcal{F}_1$ and $\mathcal{F}_2$ are minimally rigid, so is $\mathcal{F}$.

The setting described in Theorem 3 is depicted in Figure 28.5. Observe that a triangle is obviously minimally rigid. The theorem then applies identifying $\mathcal{F}_1$ with the triangle formed by A_1, A_2, and A_3 and $\mathcal{F}_2$ with the triangle formed by T_1, T_2, and T_3. In light of the minimal rigidity of the formation of Figure 28.4, there will be noncongruent formations meeting the distance constraints. Then, even though the positions of A_1, A_2, and A_3 are fixed, the positions of T_1, T_2, and T_3 will not be uniquely determinable.

28.4 FOUR-BAR LINKAGE MECHANISMS

Four-bar linkage mechanisms perform a wide variety of motions with a few simple parts. Furthermore, due to their ease of design calculations, they have gained much popularity in mechanical machine design. An example of such a mechanism is presented in Figure 28.6.

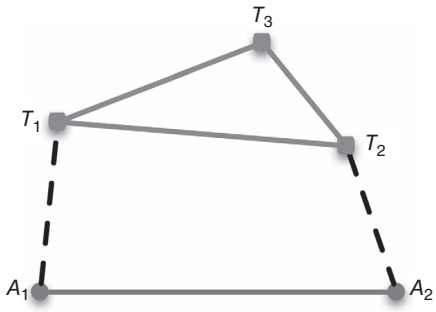

Figure 28.6 The four-bar linkage mechanism obtained after deletion of A_3T_3.

In a four-bar linkages mechanism, there is a fixed link that is called the *frame*. There are two *side links* that can revolve around the ends of the frame, and the remaining (fourth) link is called the *coupler*. A four-bar linkage mechanism is characterized by the length of each of its links, and the *configuration* of its coupler, that is, open or crossed configuration [25]. Furthermore, we have the following concepts in four-bar linkage mechanisms [26]:

- A side link that can fully revolve around (360°) the end point of the frame is called a *crank*.
- Any link that cannot fully revolve is called a *rocker*.

Although we do not use the following theorem extensively in this chapter, we present it as background information that will assist in interpreting the subsequent examples.

***Theorem 4 (Grashof's Theorem [21])*:** A four-bar mechanism has at least one crank link if and only if

$$s + l \leq p + q, \tag{28.1}$$

and all three mobile links are rockers if

$$s + l > p + q. \tag{28.2}$$

Here, l and s are the lengths of the longest link and the shortest link, respectively, and p and q are the lengths of the other two links. For example, in Figure 28.6, s and l are A_2T_2 and A_1A_2, respectively. The inequality (Eq. 28.1) is known as *Grashof's criterion*.

In the mechanism depicted in Figure 28.6, T_3, which is a fixed point on a rigid body attached to the coupler link T_1T_2, is termed the *coupler point*. The curve that this coupler point moves on in both open and cross configurations is called the *coupler curve*. Generally, coupler curves are closed curves, but for some special mechanisms we will have open coupler curves. These correspond to situations where the area enclosed by the coupler curve shrinks to zero.

A coupler curve K_C may comprise either a single part or a bipartite curve (a bipartite curve is one with two branches, like a hyperbola). In the case where K_C is bipartite, we denote the branches as K_{C_1} and K_{C_2}, where K_{C_1} is the curve obtained

by the coupler point in open configuration, and K_{C_2} is constructed by the curve in cross configuration.

For a given four-bar linkage mechanism, as in Figure 28.6, the equation of the coupler curve (bipartite or single part), K_C, where the center of Cartesian coordinates system is placed on A_1, and A_1 and A_2 are placed on the x-axis, is [21]:

$$\begin{aligned} & r_{23}^2((x-k)^2+y^2)(x^2+y^2+r_{13}^2-R_1^2)^2 \\ & -2r_{23}r_{13}((x^2+y^2-kx)\cos\eta_3+ky\sin\eta_3)(x^2+y^2+r_{13}^2-R_1^2) \\ & +((x-k)^2+y^2+r_{23}^2-R_2^2)+r_{13}^2(x^2+y^2)((x-k)^2+y^2+r_{23}^2-R_2^2)^2, \\ & -4r_{23}^2r_{13}^2((x^2+y^2-kx)\sin\eta_3-ky\cos\eta_3)^2=0 \end{aligned} \tag{28.3}$$

where k is the length of the frame link, $\overline{A_1A_2}$, $\eta_3 = \measuredangle T_1T_3T_2$, r_{ij} is the distance between agents T_i and T_j, and $R_i = d/(2\sin\lambda_i)$.

In addition, another coupler curve, K'_C, can be obtained from the reflection of K_C, when A_1A_2 is the image axis. In general, the equation describing K'_C can be obtained by substituting $-y$ for y in (28.3). In the case of a bipartite K_C, we denote the branches of K'_C as K'_{C_1} and K'_{C_2}. As a result, the locus of the coupler point is made up of two polynomial curves, each with degree of six. More specifically, we have the following result from [21] for bipartite coupler curves:

***Proposition 1*:** Bipartite coupler curves occur when and only when Grashof's criterion holds; all other cases yield coupler curves that always consist of a single part.

28.5 A LOCALIZATION ALGORITHM BASED ON FOUR-BAR LINKAGE MECHANISMS

Let us revisit the problem described in Section 28.2. It has been assumed that the agents form a triangular formation, where T_i is the ith agent, with $\mathbf{x}_i = [x_{T_i}, y_{T_i}]^{\mathrm{T}} \in \mathbb{R}^2$ as its coordinates. The distance between two agents T_i and T_j is known and equal to r_{ij} (or r_{ji}). For a given agent, T_i, and two landmarks with known positions, L_1 and L_2, the locus for the position of T_i when $\measuredangle L_1T_iL_2 = \lambda_i$ is a part of a circle denoted by $C(\mathrm{a}_i,R_i)$, where $R_i = d/2\ \sin(\lambda_i)$ is the radius of the circle and A_i is the center. Furthermore, assuming that the origin of the global coordinates frame is the middle of L_1L_2, $d = \overline{L_1L_2}$ and the x-axis coincides with the perpendicular bisector of L_1L_2, the position of A_i is considered to be $\mathrm{a}_i = [x_i,y_i]^{\mathrm{T}} = [d/2\tan\lambda_i, 0]^{\mathrm{T}}$. Note that T_i, L_1, and L_2 lie on the same circle described above.

In Figure 28.1b, each mobile platform, T_i, $i = 1,2,3$, and the associated circles are depicted. In this case, the centers of the circles, A_i, serve as the virtual anchors since we know their exact positions in the plane. Hence, the agents, T_i ($i \in \{1,2,3\}$), in the formation and these virtual anchors, A_j ($j \in \{1,2,3\}$), form a graph that satisfies

the conditions presented in Problem 1. Here, first, we make the relationship between the localization problem described in Problem 1 and the concept of four-bar linkage mechanism clear, and then using this concept we present an upper bound for the number of localization possibilities.

Note that the graph representation of Problem 1 in Figure 28.4 can be further iterated to obtain the virtual four-bar linkage mechanism representation in Figure 28.6 by representing the distance constraints on $|A_1A_2$, $|A_1T_1$, $|A_2T_2$, $|T_1T_2$ as bars, and decoupling the distance constraint on A_3T_3 from this representation. Because of this decoupled distance constraint, T_3 is on the circle $C(a_3, R_1)$ with A_3 as its center and R_1 as its radius. Hence, the possible solutions for the localization problem can be obtained from the calculation of intersections of the circle, $C(a_3, R_3)$, and the two coupler curves K_C and K'_C defined in Section 28.4.

In [22], the number of intersections of coupler curves and a circle is computed using concepts of circularity and order of the curves. The result, according to [22], in our context is as follows:

***Lemma 1*:** The circle, $C(a_3, R_3)$, and the coupler curve described by (28.3) have at least two and at most six real points of intersection.

Using Lemma 1, we establish that the maximum number of localization solutions is 12 in the following theorem:

***Theorem 5*:** The maximum number of (real) localization solutions for Problem 1 is 12. For generic values of distances and angles, the minimum number of localization solutions is four.

***Proof*:** Equation (28.3) corresponds to the coupler curves for the four-bar linkages mechanism depicted in Figure 28.6 corresponding to Problem 1 [21]. Since there are two (single-part or bipartite) coupler curves (the second one is the image of the first one when the frame link is the image axis) and for each coupler curve based on Lemma 1 there are a maximum of six and a minimum of two possible solutions, we have at most 12 possible solutions, and at least four localization solutions.

Returning to the problem presented in Section 28.2, based on the procedure introduced earlier in this section for constructing a four-bar mechanism by deleting edge A_3T_3, we can have the linkage mechanism depicted by solid lines in Figure 28.1b. In addition, here for the coupler curve equation, we have $k = (d/[2\tan\lambda_2]) - (d/[2\tan\lambda_1])$, $R_1 = d/(2\sin\lambda_1)$, and $R_2 = d/(2\sin\lambda_2)$. From Theorem 5, we can have up to 12 localization solutions. We are now ready to provide a localization algorithm to address Problem 1(ii). Algorithm 28.1 can be used to find up to twelve localization solutions (up to six pairs of mirror solutions with respect to the line connecting A_1 to A_2).

Algorithm 28.1 Three Agent and Two Landmark Localization

Find $m \leq 6$ real intersection points of (28.3) and $(x - x_3)^2 + (y - y_3)^2 - R_3^2$, $x_{3i} = [x_{iT_3}, y_{iT_3}]^T$, $i = 1, \ldots, m$.

for $i = 1$ to m **do**

Solve the system of equation for x_{T_1}, y_{T_1}, x_{T_2}, and y_{T_2}:

$$(x_{iT_3} - x_{T_1})^2 + (y_{iT_3} - y_{T_1})^2 - r_{13}^2 = 0$$

$$(x_{iT_3} - x_{T_2})^2 + (y_{iT_3} - y_{T_2})^2 - r_{23}^2 = 0$$

$$(x_{T_2} - x_{T_1})^2 + (y_{T_2} - y_{T_1})^2 - r_{12}^2 = 0$$

$$(x_1 - x_{T_1})^2 + (y_1 - y_{T_1})^2 - R_1^2 = 0$$

$$(x_2 - x_{T_2})^2 + (y_2 - y_{T_2})^2 - R_2 = 0$$

$$s_i \leftarrow [x_{T_1}, y_{T_1}, x_{T_2}, y_{T_2}, x_{iT_3}, y_{iT_3}] \quad s_i' \leftarrow [x_{T_1}, -y_{T_1}, x_{T_2}, -y_{T_2}, x_{iT_3}, -y_{iT_3}]$$

end for

Return S and S′ as the sets of $2m$ localization solutions where s_i and s_i' are their rows, respectively.

Example 28.1 Simulations with Three Agents and Two Landmarks

The angle and distance values used in each simulation scenario are presented in Table 28.1. In addition, it is worth mentioning that after running several simulations, a case with 12 localization solutions was never encountered.

The important characteristics of each simulation result and the number of localization solutions in each scenario are presented in Table 28.2. The legends used in the simulation results are described in Table 28.3. In Figures 28.7 and 28.8, two scenarios where, respectively, four and eight localization solutions exist are presented. A nongeneric case is presented in Figure 28.9a, where there are repeated localization solutions. A bad geometry is identified in Figure 28.9b, where an infinite number of localization solutions exists. This infinite localization ambiguity occurs if the three sensors and the two landmarks lie on a common circle. Invalid localization solutions occur in the scenario that is depicted in Figure 28.10a. Another nongeneric case arises when the angles subtended at any two of the agents by the landmarks are equal, and this is depicted in Figure 28.10b. Note that for all the scenarios the landmarks L_1 and L_2 are placed at $[0,1]^T$ and $[0,-1]^T$, respectively.

TABLE 28.1. The Angle and Distance Values in Each Scenario

Scenario	λ_1 (rad)	λ_2 (rad)	λ_3 (rad)	$\overline{T_1T_2}$ (m)	$\overline{T_1T_3}$ (m)	$\overline{T_2T_3}$ (m)
Figure 28.7	1.0472	0.6283	0.5236	1	1	1
Figure 28.8	0.3805	0.2526	0.1674	3.1623	5.099	2.8284
Figure 28.9a	1.0472	0.8976	0.7854	1.5	0.9765	1.25
Figure 28.9b	0.2487	0.2487	0.2487	2.0859	2.7552	4.6188
Figure 28.10a	0.7854	0.6283	0.5236	3	2	2
Figure 28.10b	0.7854	0.7854	0.5236	1	1	1

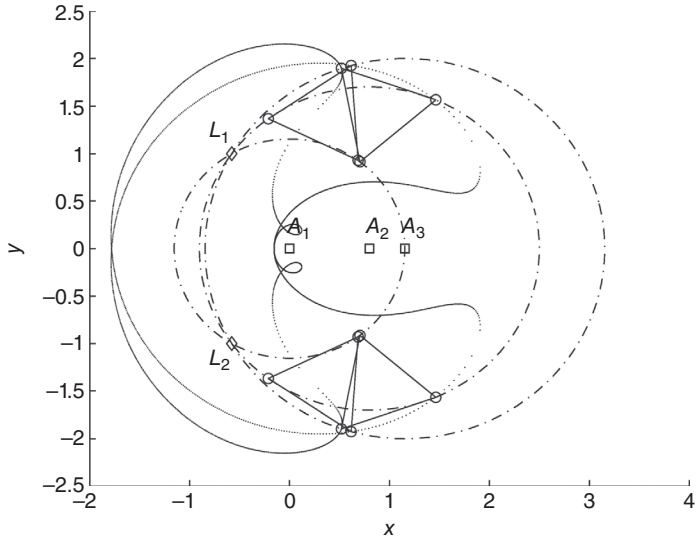

Figure 28.7 The possible localization solutions for scenario 1.

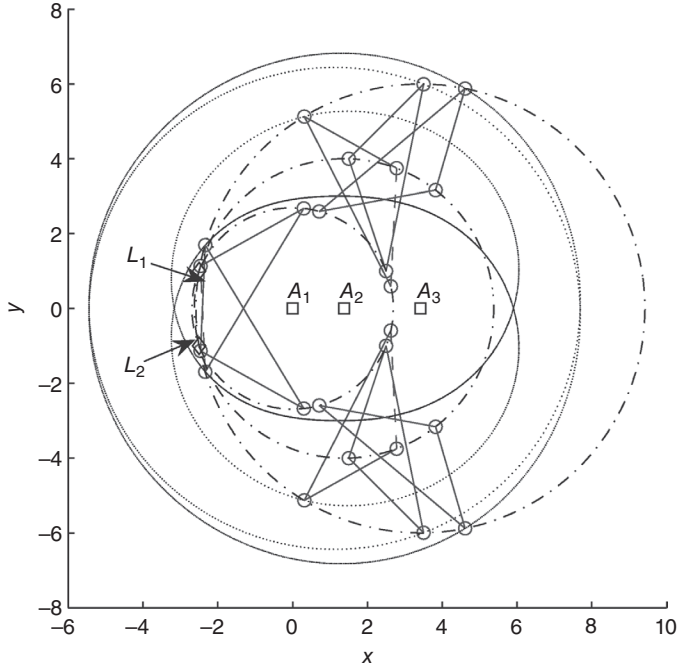

Figure 28.8 The possible localization solutions for scenario 2.

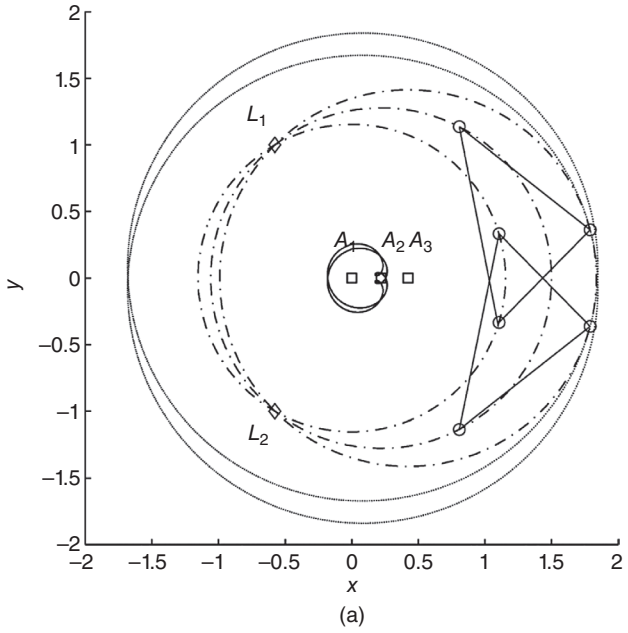

(a)

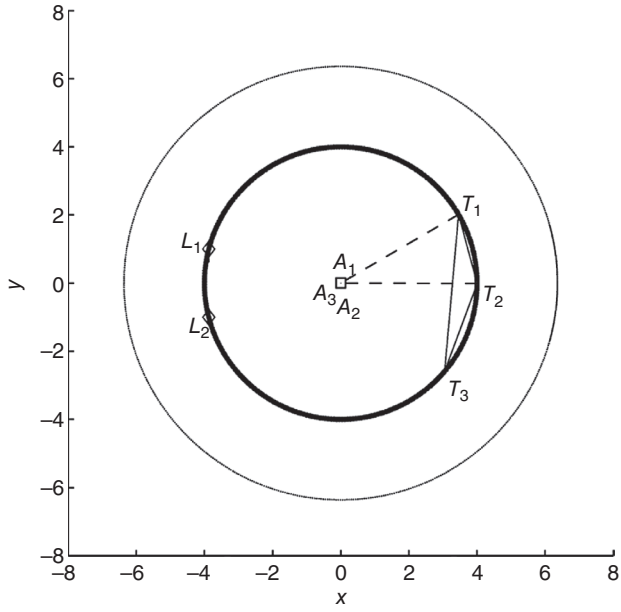

(b)

Figure 28.9 Simulation results. (a) Repeated localization solutions (scenario 3 as described in Table 28.2). (b) Infinite number of localization solutions for scenario 4 as described in Table 28.2. The locus of T_3 coincides with one of the branches of the coupler curve.

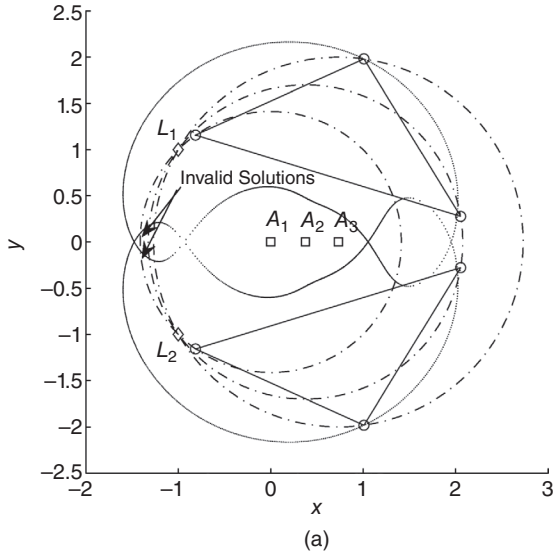

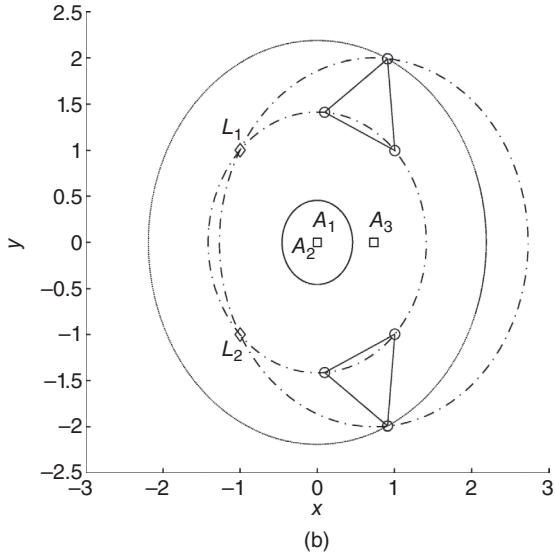

Figure 28.10 Simulation results. (a) Occurrence of invalid localization solutions (scenario 5 as described in Table 28.2). (b) Localization solutions shen two subtended angles λ_1 and λ_2 are equal (scenario 6 as described in Table 28.2)

TABLE 28.2. The Number of Localization Solutions in Each Scenario and Important Characteristics of Each Scenario

Scenario	No. of Distinct Solutions	Characteristic
1 (Fig. 28.7)	4	Generic
2 (Fig. 28.8)	8	Generic
3 (Fig. 28.9a)	2	Nongeneric/repeated solutions
4 (Fig. 28.9b)	Infinite	Nongeneric/infinite ambiguity
5 (Fig. 28.10a)	2	Generic/invalid solutions
6 (Fig. 28.10b)	2	Nongeneric/two equal angles

TABLE 28.3. The Legends Used in Simulation Results

Agent	Small solid circle
Landmark	Solid diamond
Formation	Solid triangles
Agent locus	Dashed circles
Coupler curve	Dotted curves

28.6 LOCALIZATION OF LARGER FORMATIONS

The methodology presented in the previous sections can be extended to localization of certain formations having more than three agents, as will be elaborated in what follows. The following theorem gives the maximum possible number of solutions for formations with globally rigid underlying graphs:

***Theorem 6*:** Consider a formation $\mathcal{F}$ with the underlying globally rigid graph $\mathcal{G}(\mathcal{V}, \mathcal{E})$, and the three agents, T_1, T_2, and T_3, in the formation that form a triangle. Assuming that these three agents are the only agents capable of measuring the angle subtended at them by the two landmarks L_1 and L_2, with known positions, then there are at most 12 possible localization solutions for the formation.

***Proof*:** Theorem 5 states that the upper bound for the number of localization solutions of a triangular formation using the value of the angles subtended at each agent by two landmarks is 12. On the other hand, in [20], it has been shown that the necessary and sufficient condition for unique localization of a formation is that the associated graph is globally rigid and there are three nodes with exactly known positions. As a result, for each possible localization of three agents, there is a localization solution for the whole formation, so there are up to 12 possible localization possibilities for the formation.

Now, assume that we have another agent, T_4, that can measure its distance from agents T_1, T_2, and T_3 and the angle subtended at itself by the two landmarks, λ_4. Knowing this angle, we can characterize another anchor node, A_4 with known position, similar to A_1, A_2, and A_3, for the time being assuming that A_i are not collinear. We can calculate the distance between T_4 and A_4. A_i, $i = 1, \ldots, 4$, form a complete (and therefore globally rigid) graph, and we already have implicitly assumed that T_1, T_2, T_3, and T_4 also form a complete graph. We know from [27] that by connecting a globally rigid graph to another one using four edges, the resulting graph is globally

rigid as well, and as a result, for generic positions of the agents there is a unique realization. Thus, the formation described above has a unique localization solution for generic positions of agents and landmarks, and it is the addition of an agent capable of measuring the angle subtended at itself by the two landmarks that disambiguates the multiple localization solutions. However, the important point here is that the anchor nodes A_1, A_2, A_3, and A_4 are collinear, which violates genericity. This collinearity results in having mirror localization solutions at different sides of the line that the anchors are placed on.

We conclude this section with the following remark, which is an extension of Theorem 5:

***Remark 2*:** Consider a formation F with the underlying globally rigid graph $\mathcal{G}(\mathcal{V},\mathcal{E})$, and the four agents, T_1, T_2, T_3, and T_4, in the formation that form a complete graph. Assuming that these four agents are the only agents capable of measuring the angle subtended at them by the two landmarks L_1 and L_2, with known positions, it can be shown that there are at most two possible localization solutions for the formation.

Example 28.2

Consider four agents T_i, $i = 1, \ldots, 4$, at unknown positions with $\lambda_1 = 1.4407$, $\lambda_2 = 1.3051$, $\lambda_3 = 0.9193$, $\lambda_4 = 0.8635$, $\overline{T_1T_2} = 0.4310$, $\overline{T_1T_3} = 0.6236$, $\overline{T_1T_4} = 0.9402$, $\overline{T_2T_3} = 0.9481$, $\overline{T_2T_4} = 0.7957$, $\overline{T_3T_4} = 0.9306$, $L_1 = (0,1)^{\mathrm{T}}$, and $L_2 = [0,-1]^{\mathrm{T}}$. The two possible positions for the agents are depicted in Figure 28.11. A simple way to calculate these solutions is to use Algorithm 28.1 to find a set of possible solutions for the positions of T_1, T_2, and T_3. Calculate a candidate solution for the position of T_4 using the interagent distances for each of these solutions sets, and discard all the solutions that are not consistent with the angle measurements associated with T_4.

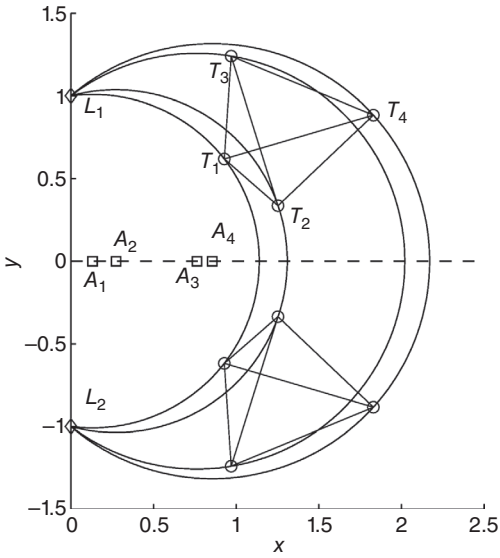

Figure 28.11 The possible localization solutions where four agents measure the subtended angle by the landmarks.

28.7 LOCALIZATION WITH EXTRA LANDMARKS

In this section, we consider the cases where bearing measurements from another landmark are available. Suppose another landmark, L_3, is positioned at a known position in the plane, and further imagine that agent T_1 can measure the subtended angle by landmarks L_1 and L_2, L_1 and L_3, and L_2 and L_3. These three angle measurements result in having three circles with the common point of intersection exactly at T_1 for generic positions for T_1. Hence, having another landmark generically disambiguates the multiple localization solutions.

There are certain geometries for which a unique solution for the agent cannot be obtained; for instance, if the agent is located on the circumcircle of the triangle $\Delta L_1L_2L_3$ one cannot localize it. In what follows, we address the problem of localization of a formation of three agents measuring the subtended angle at them by three landmarks in the presence of noise.

When there are three agents and two landmarks, there is no special technique for dealing with the noise. One simply proceeds using noisy measurements in lieu of noiseless measurements. However, when the noiseless equations are overdetermined, as for example with three landmarks, a modified method is required to handle the equations, temporarily assuming there is no measurement noise. As described before for each agent and any selection of two landmarks, we can define a circle. Call the center and the radius of the circle defined by T_i, L_1, and L_2 $\mathrm{a}_i = [x_i,y_i]^{\mathrm{T}}$ and R_i, respectively; term the center and the radius of the circle defined by T_i, L_1, and L_3 $a_i' = [x_i', y_i']^{\mathrm{T}}$ and R_i', and term the center and the radius of the circle defined by T_i, L_2, and L_3, $a_i'' = [x_i'', y_i'']^{\mathrm{T}}$ and R_i''. All the equations that govern the system can be written as

$$\begin{aligned}
(x_{T_i} - x_i)^2 + (y_{T_i} - y_i)^2 - R_i^2 = 0, \quad & i \in \{1,2,3\} \\
(x_{T_i} - x_i')^2 + (y_{T_i} - y_i')^2 - R_i'^2 = 0, \quad & i \in \{1,2,3\} \\
(x_{T_i} - x_i'')^2 + (y_{T_i} - y_i'')^2 - R_i''^2 = 0, \quad & i \in \{1,2,3\} \\
(x_{T_i} - x_{T_j})^2 + (y_{T_i} - y_{T_j})^2 - R_{ij}^2 = 0, \quad & i,j \in \{1,2,3\}
\end{aligned} \qquad (28.4)$$

where $x_{T_i} = [x_{T_i}, y_{T_i}]^{\mathrm{T}}$ is the position of agent T_i. It is obvious that (28.4) has a unique set of solutions for the positions of the T_i. This solution is a root of the following polynomial.

$$\begin{aligned}
P = & \sum_{i=1}^{3} \left((x_{T_i} - x_i)^2 + (y_{T_i} - y_i)^2 - R_i^2\right)^2 \\
& + \sum_{i=1}^{3} \left((x_{T_i} - x_i')^2 + (y_{T_i} - y_i')^2 - R_i'^2\right)^2 \\
& + \sum_{i=1}^{3} \left((x_{T_i} - x_i'')^2 + (y_{T_i} - y_i'')^2 - R_i''^2\right)^2 \\
& + \sum_{i,j \in \{1,2,3\}} \left((x_{T_i} - x_{T_j})^2 + (y_{T_i} - y_{T_j})^2 - R_{ij}^2\right)^2
\end{aligned} \qquad (28.5)$$

Furthermore, it is easy to show that this solution is the global minimizer of (28.5) as well. So the solution $\hat{\mathbf{x}}\boldsymbol{T} = [\hat{\mathbf{x}}_{T_1}^{\mathrm{T}}, \hat{\mathbf{x}}_{T_2}^{\mathrm{T}}, \hat{\mathbf{x}}_{T_3}^{\mathrm{T}}]^{\mathrm{T}}$ is obtained by

$$\hat{\mathbf{x}}_T = \operatorname{argmin} P. \tag{28.6}$$

Now assume that the measurement is noisy, hence (28.4) does not necessarily have a solution; however, in the light of the introduction of (28.5), one can solve the minimization equation to obtain an estimate for the solution. There are readily available software packages that enable us to minimize such cost functions, for example, Reference [28]. In the next section, we introduce some numerical simulations that illustrate the applicability of the methods introduced in this chapter to some possible scenarios.

Example 28.3 Simulations with Three Agents and Three Landmarks

Here we consider that three landmarks are placed at $[-1,0]^{\mathrm{T}}$, $[1,0]^{\mathrm{T}}$, and $[0,0]^{\mathrm{T}}$. The exact position of agents 1, 2, and 3 are, respectively, $[3,6]^{\mathrm{T}}$, $[5,8]^{\mathrm{T}}$, and $[2,3]^{\mathrm{T}}$ (the positions are in meters). We consider that interagent distance measurements are corrupted by a Gaussian noise with a variance equal to $0.25\,\mathrm{m}^2$, and the angle measurements are corrupted by a Gaussian noise with a variance equal to $0.0005\ \mathrm{rad}^2$. Running the simulation for 20 times and solving (28.6), we obtain $\overline{\mathbf{x}}_{T_1} = [2.9492, 5.9528]^{\mathrm{T}}$, $\overline{\mathbf{x}}_{T_2} = [4.9306, 7.9594]^{\mathrm{T}}$, and $\overline{\mathbf{x}}_{T_1} = [1.9290, 2.9609]^{\mathrm{T}}$ as average values for the positions of T_1, T_2, and T_3, respectively. As is clear, the average estimates are very close to the actual values. Furthermore, the variances of all the solutions for the x coordinates of T_1, T_2, and T_3 are 0.0267, 0.0466, and 0.0443, and the variances of all the solutions for the y coordinates of T_1, T_2, and T_3 are 0.0155, 0.0095, and 0.0097, respectively. We have used Gloptipoly 3 [28] to solve the optimization problem generated from this scenario.

28.8 AVAILABILITY OF MORE ANGLE MEASUREMENTS FOR THREE AGENTS

So far, in this chapter, each agent is assumed to be able to detect the subtended angle by the landmarks at them only and not to be able to measure relative bearings to other agents or to one agent and one landmark. This scenario is more common if the agents are equipped with dedicated RF angle-of-arrival devices that measure bearings to transmitting beacons or detect other signals transmitted by other RF emitters of opportunity such as broadcast TV. Another scenario is that some or all agents have optical on-board sensors with a narrow field of view. In this case, the agents may not necessarily have other agents within their sensor field of view. However, use of, for example, a 360° camera sensor gives rise to a different scenario where the agents in the formation are capable of measuring not only the angle subtended by the landmarks at them but also the angle subtended at them by any pair of the agents or the landmarks.

In this section, we briefly consider this latter scenario, in which (as before) there are three agents and two landmarks. For agent T_i, we denote the angle

subtended by L_k and agent T_j, μ^i_{jk}, and the angle subtended by T_j and T_k by η_i. Measurements of these subtended angles as well as λ_i, as before, make it possible to localize up to two possible positions. We formally show this in the following theorem.

***Theorem 7*:** Knowing all the angles λ_i, $i = 1,2,3$, η_i, $i = 1,2,3$, and $\mu^i_{k,j}$, $k = 1,2$, $i,j = 1,2,3$ and the positions of landmarks L_1 and L_2, one can find two solutions for the position of the agents T_i, $i = 1,2,3$, which are reflections through the line connecting the landmarks.

***Proof*:** Consider a polygon with vertices defined by T_i, $i = 1,2,3$, and L_j, $j = 1,2$. By all the angles λ_i, $i = 1,2,3$, η_i, $i = 1,2,3$, and $\mu^i_{k,j}$, $k = 1,2$, $i,j = 1,2,3$, we can characterize all similar polygons with the same angles. Furthermore, knowing the distance between L_1 and L_2 fixes the scale of the polygon, knowing the position of either L_1 or L_2 fixes the two-dimensional translation, and knowing the position of the other landmark fixes the orientation of the polygon; and hence, the solution set is composed of up to two polygons that can be constructed via symmetry from each other, where L_1L_2 is the mirror axis.

***Remark 3*:** Since we have already fixed on which side of L_1L_2 the formation is located, the only possibility is the polygon on the a priori known side of L_1L_2.

We conclude this section by the following example.

Example 28.4

Consider three agents T_i, $i = 1, \ldots, 3$, at unknown positions with $\lambda_1 = 0.2075$, $\lambda_2 = 0.1419$, $\lambda_3 = 0.0821$, $\eta_1 = 0.1419$, $\eta_2 = 2.8890$, and $\eta_3 = 0.1107$, $\mu^1_{1,2} = 2.8023$, $\mu^1_{1,3} = 2.9442$, $\mu^1_{2,1} = 2.5948$, $\mu^1_{2,3} = 2.7367$, $\mu^2_{1,1} = 0.1419$, $\mu^2_{1,3} = 3.0309$, $\mu^2_{2,1} = 0.2838$, $\mu^2_{2,3} = 3.1104$, $\mu^3_{1,1} = 0.0476$, $\mu^3_{1,2} = 0.0631$, $\mu^3_{2,1} = 0.1297$, $\mu^3_{2,1} = 0.0190$, $L_1 = (0,1)^T$, and $L_2 = [0,-1]^T$. Using elementary geometric arguments one can calculate all the angles of the pentagon formed by T_1, T_2, T_2, L_1, and L_4. Using these angles along with the exact positions of L_1 and L_2, one can calculate two mirrored solutions with L_1L_2 as the reflection axis for the target positions. The two possible sets of positions for the agents are $T_1 = [\pm 2,4]^T$, $T_2 = [\pm 6,7]^T$, and $T_3 = [\pm 10,12]^T$.

28.9 CONCLUSIONS

In this chapter, we have demonstrated that there are up to 12 possible localization solutions to the problem of localization of a formation composed of three agents, collecting bearing measurements to two landmarks at known positions and measuring their interagent distances. Furthermore, we extend this result to a more general case where a larger formation is to be localized using the same information as before. In addition, the effect of having extra landmarks on the number of the solutions to the problem was studied as well, and in this case a method to improve the accuracy of the localization solution was proposed. Some simulation results were presented to show the applicability of the methods. In the end, we briefly considered another closely

related localization problem, where the agents can measure all the subtended angles at them, and show the uniqueness of the localization for this case.

ACKNOWLEDGMENTS

This work is supported by NICTA, which is funded by the Australian government as represented by the Department of Broadband, Communications, and the Digital Economy, and the Australian Research Council through the ICT Centre of Excellence program.

REFERENCES

[1] P. W. Ward, "GPS receiver RF interference monitoring, mitigation and analysis techniques," *Navigation*, vol. 41, pp. 367–391, 1994–1995.

[2] G. Dedes and A. G. Dempste, "Indoor GPS positioning: Challenges and opportunities," *IEEE Conf. on Vehicular Technology*, Dallas, TX, Sep. 2005, pp. 412–415.

[3] A. H. Sayed and A. Tarighat, "Network-based wireless location," *IEEE Signal Process. Mag.*, vol. 22, pp. 24–40, 2005.

[4] M. Cao, B. D. O. Anderson, and A. S. Morse, "Sensor network localization with imprecise distances," *Syst. Control Lett.*, vol. 55, pp. 887–893, 2006.

[5] P. Stoica and J. Li, "Source localization from range-difference measurements," *IEEE Signal Process. Mag.*, vol. 23, pp. 63–65, 69, 2006.

[6] I. Shimshoni, "On mobile robot localization from landmark bearings," *IEEE Trans. Rob. Autom.*, vol. 13, pp. 971–976, 2002.

[7] M. Betke and L. Gurvits, "Mobile robot localization using landmarks," *IEEE Trans. Rob. Autom.*, vol. 13, pp. 251–263, 1997.

[8] H. Hmam, "Mobile platform self-localisation," in *Proc. of Information Decision and Control*, Adelaide, Australia, Feb. 2007, pp. 242–247.

[9] J. S. Esteves, A. Carvalho, and C. Couto, "Generalized geometric triangulation algorithm for mobile robot absolute self-localization," in *IEEE Int. Symp. on Industrial Electronics*, Rio de Janeiro, Brasil, Jun. 2003, pp. 346–351.

[10] J. Ryde and H. Hu, "Fast circular landmark detection for cooperative localisation and mapping," in *Int. Conf. on Robotics and Automation*, Barcelona, Spain, Apr. 2005, pp. 2745–2750.

[11] T. Eren, D. Goldenberg, W. Whiteley, Y. Yang, A. S. Morseand, and B. D. O. Anderson, "Rigidity, computation and randomization in network localization," in *Proc. of Network Localization, Joint Conf. of IEEE Computer and Communication Societies*, Hong Kong, Mar. 2004, pp. 2673–2684.

[12] S. I. Roumeliotis and G. A. Bekey, "Collective localization: A distributed Kalman filter approach to localization of groups of mobile robots," in *Proc. of Int. Conf. on Robotics and Automation*, San Francisco, CA, Apr. 2000, pp. 2958–2965.

[13] N. M. Kwok, G. Dissanayake, and Q. P. Ha, "Bearing-only SLAM using a SPRT based Gaussian sum filter," in *Proc. of Int. Conf. on Robotics and Automation*, Barcelona, Spain, Apr. 2005, pp. 1109–1114.

[14] G. Laman, "On graphs and rigidity of plane skeletal structures," *J. Engrg. Math.*, vol. 11, pp. 331–340, 1970.

[15] T. Tay and W. Whiteley, "Generating isostatic frameworks," *Struct. Topology*, vol. 11, pp. 21–69, 1985.

[16] B. D. O. Anderson, C. Yu, B. Fidan, and J. M. Hendrickx, "Rigid graph control architectures for autonomous formations," *IEEE Control Syst. Mag.*, vol. 28, pp. 48–63, 2008.

[17] C. Yu, B. Fidan, J. M. Hendrickx, and B. D. O. Anderson, "Merging multiple formations: A meta-formation prospective," in *Proc. of CDC 2006*, San Diego, CA, Dec. 2006, pp. 4657–4663.

[18] G. Mao, B. Fidan, and B. D. O. Anderson, "Localization," in *Sensor Networks and Configuration: Fundamentals, Techniques, Platforms and Experiments*, New York: Springer, 2006, ch. 13.
[19] B. Hendrickson, "Conditions for graph unique realizations," *SIAM J. Comput.*, vol. 21, pp. 65–84, 1992.
[20] B. Jackson and T. Jordan, "Connected rigidity matroids and unique realizations of graphs," *J. Comb. Theory B*, vol. 94, pp. 1–29, 2005.
[21] R. Beyer, *Kinematic Synthesis of Mechanisms,* Translated from German by H. Kuenzel. London: Chapman & Hall, 1963.
[22] W. Chung, "The characteristics of a coupler curve," *Mech. Mach. Theory*, vol. 40, no. 10, pp. 1099–1106, 2005.
[23] D. K. Goldenberg, A. Krishnamurthy, W. C. Maness, Y. R. Yang, A. Young, A. S. Morse, A. Savvides, and B. D. O. Anderson, "Network localization in partially localizable networks," in *Proc. IEEE INFOCOM 2005. 24th Annual Joint Conf. of the IEEE Computer and Communications Societies*, 2005, pp. 313–326.
[24] W. T. Tutte, "A theory of 3-connected graphs," *Indagationes Math.*, vol. 23, pp. 441–455, 1961.
[25] R. L. Norton, *Design of Machinery*. New York: McGraw-Hill, 1992.
[26] Y. Zhang, S. Finger, and S. Behrens, "Rapid design through virtual and physical prototyping," Carnegie Mellon University. Available: http://www.cs.cmu.edu/~rapidproto/mechanisms/chpt5.html
[27] C. Yu, B. Fidan, and B. D. O. Anderson, "Principles to control autonomous formation merging," in *Proc. of American Control Conf.*, Minneapolis, MN, Jun. 2006, pp. 762–768.
[28] D. Henrion, J. B. Lasserre, and J. Loefberg, "Gloptipoly 3: Moments, optimization and semidefinite programming," *Optim. Methods Softw.*, vol. 24, p. 761, 2009.